

---

---

---

---

---

---

---

**Förster Resonance Energy Transfer**  
**FRET**

I should note before we start that the Merriam-Webster online dictionary defines “FRET” as:  
**“to cause to suffer emotional strain”**

Some of these slides were prepared by Pierre Moens

---

---

---

---

---

---

---

This sentence appears in a 2006 book! Let's correct this mistake!

More than 50 years ago, the German scientist Förster discovered that close proximity of two chromophores changes their spectral properties in predictable ways (Förster, 1948a).

**Milestones in the Theory of Resonance Energy Transfer**

1922 G. Cario and J. Franck demonstrate that excitation of a mixture of mercury and thallium atomic vapors with 254nm (the mercury resonance line) also displayed thallium (sensitized) emission at 535nm.

1924 E. Gaviola and P. Pringsham observed that an increase in the concentration of fluorescein in viscous solvent was accompanied by a progressive depolarization of the emission.

1925 J. Perrin proposed the mechanism of resonance energy transfer

1928 H. Kallmann and F. London developed the quantum theory of resonance energy transfer between various atoms in the gas phase. The dipole-dipole interaction and the parameter  $R_0$  are used for the first time

1932 F. Perrin published a quantum mechanical theory of energy transfer between molecules of the same specie in solution. Qualitative discussion of the effect of the spectral overlap between the emission spectrum of the donor and the absorption spectrum of the acceptor

1946-1949 T. Förster develop the first complete quantitative theory of molecular resonance energy transfer

---

---

---

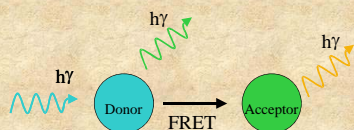
---

---

---

---

What is FRET ?



When the donor molecule absorbs a photon, and there is an acceptor molecule close to the donor molecule, radiationless energy transfer can occur from the donor to the acceptor.

FRET results in a decrease of the fluorescence intensity and lifetime of the donor probe. It enhance the fluorescence of the acceptor probe when the acceptor is fluorescent.

PM

---

---

---

---

---

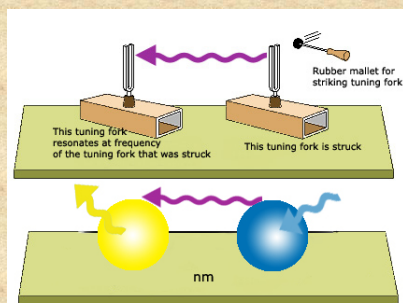
---

---

---

## Tuning fork analogy for resonance energy transfer

FRET



TV

---

---

---

---

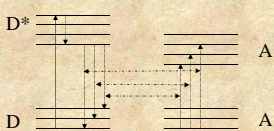
---

---

---

---

## Simplified FRET Energy Diagram



Coupled transitions

Suppose that the energy difference for one of these possible deactivation processes in the donor molecule matches that for a possible absorption transition in a nearby acceptor molecule. Then, with sufficient energetic coupling between these molecules (overlap of the emission spectrum of the donor and absorption spectrum of the acceptor), both processes may occur simultaneously, resulting in a transfer of excitation from the donor to the acceptor molecule



The interaction energy is of a dipole-dipole nature and depends on the distance between the molecules as well as the relative orientation of the dipoles

PM

---

---

---

---

---

---

---

---

### Dipole-dipole interaction



The rate of transfer ( $k_T$ ) of excitation energy is given by:

$$k_T = (1/\tau_d)(R_0/r)^6$$

Where  $\tau_d$  is the fluorescence lifetime of the donor in the absence of acceptor,  $r$  the distance between the centers of the donor and acceptor molecules and  $R_0$  the Förster critical distance at which 50% of the excitation energy is transferred to the acceptor and can be approximated from experiments independent of energy transfer.

---

---

---

---

---

---

---

---

### Förster critical distance

$$R_0 = 0.2108 (n^{-4} Q_d \kappa^2 J)^{1/6} \text{ \AA}$$

$\uparrow \quad \uparrow \quad \uparrow \quad \uparrow$   
 $n \quad Q_d \quad \kappa^2 \quad J$

$n$  is the refractive index of the medium in the wavelength range where spectral overlap is significant (usually between 1.2-1.4 for biological samples)

$Q_d$  is the fluorescence quantum yield of the donor in absence of acceptor (i.e. number of quanta emitted / number of quanta absorbed)

$\kappa^2$  (pronounced "kappa squared") is the orientation factor for the dipole-dipole interaction

$J$  is the normalized spectral overlap integral [ $\epsilon(\lambda)$  is in  $M^{-1} cm^{-1}$ ,  $\lambda$  is in nm and  $J$  units are  $M^{-1} cm^{-1} (nm)^4$ ]

---

---

---

---

---

---

---

---

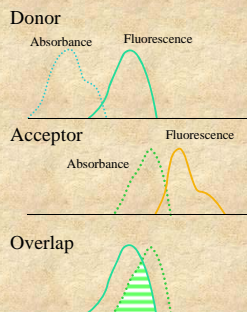
### The overlap integral $J$ is defined by:

$$J = \int_0^\infty I_D(\lambda) \epsilon_A(\lambda) \lambda^4 d\lambda$$

Where  $\lambda$  is the wavelength of the light,  $\epsilon_A(\lambda)$  is the molar absorption coefficient at that wavelength and  $I_D(\lambda)$  is the fluorescence spectrum of the donor normalized on the wavelength scale:

$$I_D(\lambda) = \frac{F_{D\lambda}(\lambda)}{\int_0^\infty F_{D\lambda}(\lambda) d\lambda}$$

Where  $F_{D\lambda}(\lambda)$  is the donor fluorescence per unit wavelength interval




---

---

---

---

---

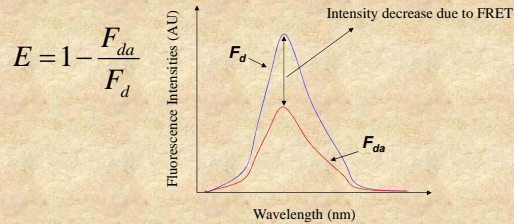
---

---

---

### Determination of the efficiency of energy transfer ( $E$ )

**Steady state method:** Decrease in donor fluorescence. the fluorescence intensity of the donor is determined in absence and presence of the acceptor.




---

---

---

---

---

---

---

---

### Determination of the efficiency of energy transfer ( $E$ )

**Time-resolved method:** Decrease in the lifetime of the donor

If the fluorescence decay of the donor is a single exponential then:

$$E = 1 - \frac{\tau_D}{\tau_D^0}$$

Where  $\tau_D$  and  $\tau_D^0$  are the lifetime of the donor in the presence and absence of acceptor, respectively

---

---

---

---

---

---

---

---

### Determination of the efficiency of energy transfer ( $E$ )

If the donor fluorescence decay in absence of acceptor is not a single exponential (probably resulting from heterogeneity of the probe's microenvironment), then it may be modeled as a sum of exponential and the transfer efficiency can be calculated using the average decay times of the donor in absence and presence of acceptor:

$$E = 1 - \frac{\langle \tau_D \rangle}{\langle \tau_D^0 \rangle}$$

Where  $\langle \tau \rangle$  is the amplitude-average decay time and is defined as:

$$\langle \tau \rangle = \frac{\sum_i \alpha_i \tau_i}{\sum_i \alpha_i}$$

---

---

---

---

---

---

---

---

### The distance dependence of the energy transfer efficiency ( $E$ )

$$r = \left( \frac{1}{E} - 1 \right)^{1/6} R_0$$

Where  $r$  is the distance separating the donor and acceptor fluorophores,  $R_0$  is the Förster distance.

Many equivalent forms of this equation is found in the literature, such as:

$$E = R_0^6 / (R_0^6 + r^6) \quad \text{or} \quad E = 1 / [1 + (r/R_0)^6]$$

---

---

---

---

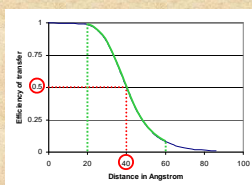
---

---

---

---

### The distance dependence of the energy transfer efficiency ( $E$ )



The efficiency of transfer varies with the inverse sixth power of the distance.

$R_0$  in this example was set to 40 Å. When the  $E$  is 50%,  $R=R_0$ .

Distances can usually be measured between  $0.5 R_0$  and  $\sim 1.5 R_0$ . Beyond these limits, we can often only say that the distance is smaller than  $0.5 R_0$  or greater than  $1.5 R_0$ . If accurate distance measurement is required then a probe pair with a different  $R_0$  is necessary.

---

---

---

---

---

---

---

---

### How was FRET theory tested experimentally?

Energy Transfer. A System with Relatively Fixed Donor-Acceptor Separation JACS 87:995(1965)

S. A. Latt, H. T. Chung, and E. R. Blout

Contribution from the Department of Biological Chemistry, Harvard Medical School, Boston, Massachusetts. Received August 24, 1964

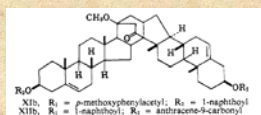


Table III

Compound	$\bar{\nu}_s$	$R_{\text{calc}}, \text{\AA}$	$R_{\text{meas}}, \text{\AA}$ (from Dreyling models), $\text{\AA}$
XI	$\bar{\nu}_s$	$21.3 \pm 1.6$	$21.8 \pm 2.0$ (linear av.)
			$19.2 \pm 2.0$ ( $(1/R)^{-1}$ )
XII	$\bar{\nu}_s$	$16.7 \pm 1.4$	$21.5 \pm 2.0$ (linear av.)
			$19.4 \pm 2.0$ ( $(1/R)^{-1}$ )

The most likely explanation for this discrepancy between the predicted and observed transfer in compound XII is that the value of the average orientation factor is greater than the estimate of  $1/3$  which was used to calculate the predicted separation.

---

---

---

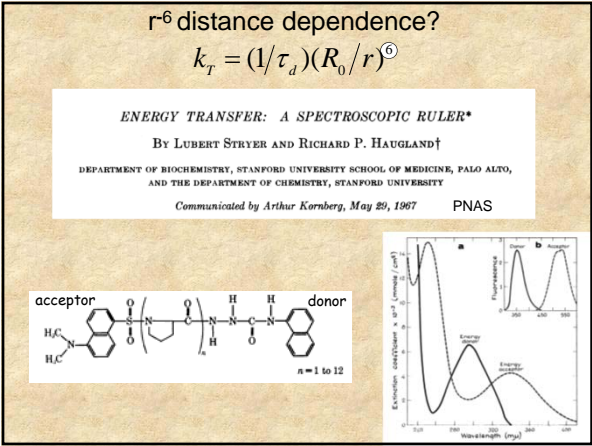
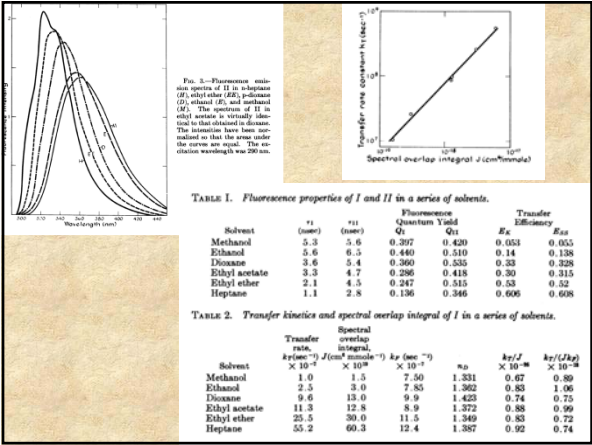
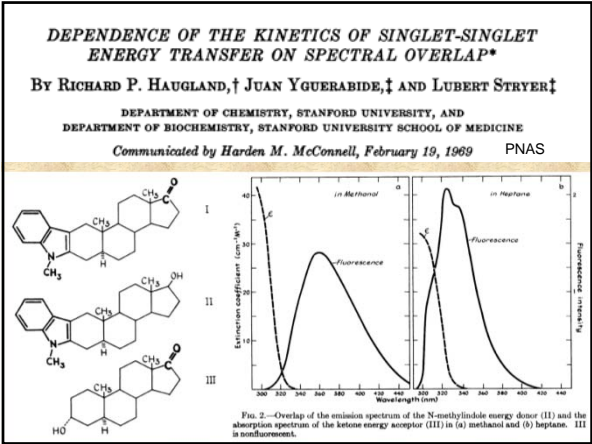
---

---

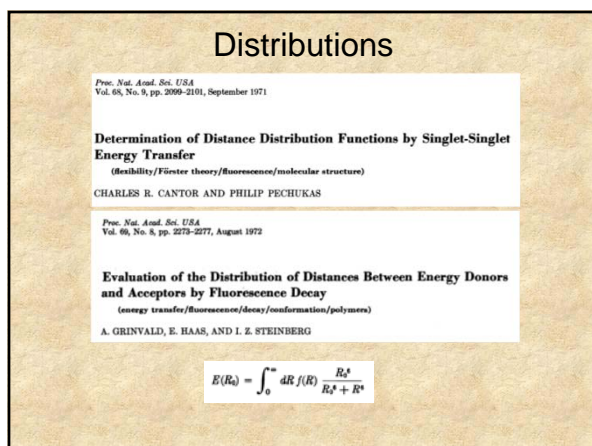
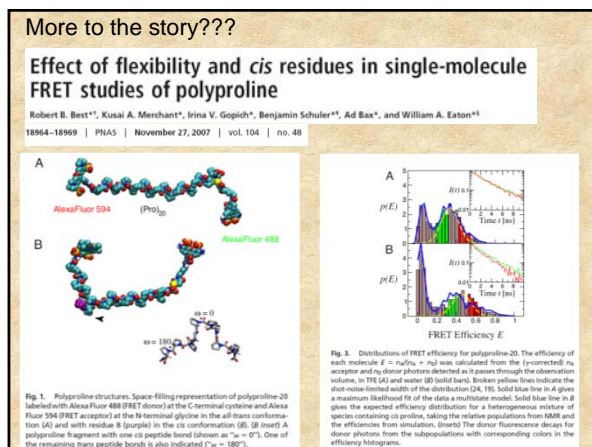
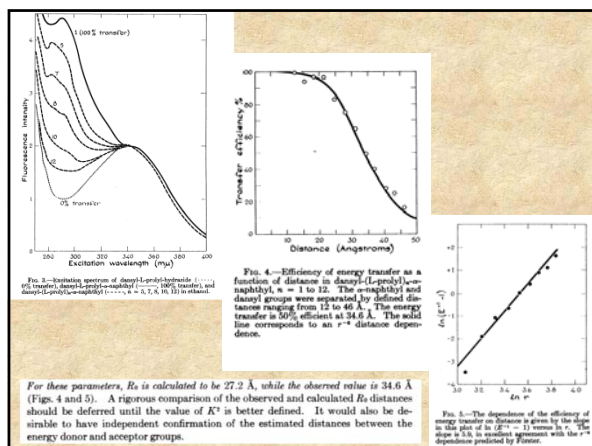
---

---

---







## Distributions

Proc. Natl. Acad. Sci. USA  
Vol. 72, No. 5, pp. 1807-1811, May 1975

### Distribution of End-to-End Distances of Oligopeptides in Solution as Estimated by Energy Transfer (Fluorescence decay/information)

ELISHA HAAS, MEIR WILCHEK, EPHRAIM KATCHALSKI-KATZIR, AND ISHAK Z. STEINBERG

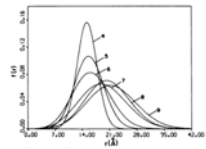
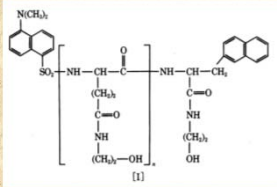


FIG. 4. The distribution function of the distances between donor and acceptor for the series of oligopeptides I,  $s = 4, 5, 6, 7, 8$ , and  $9$ . The numbers in the figure refer to the values of  $s$ .

## Distributions

Biochemistry 1988, 27, 9149-9160

9149

### Distance Distributions in Proteins Recovered by Using Frequency-Domain Fluorometry. Applications to Troponin I and Its Complex with Troponin C<sup>1</sup>

Joseph R. Lakowicz,<sup>1,2</sup> Ignacy Gryczynski,<sup>1,3</sup> Herbert C. Cheung,<sup>1</sup> Chien-Kao Wang,<sup>1</sup> Michael L. Johnson,<sup>1</sup> and Nanda Jishi<sup>1</sup>

5238

Biochemistry 1991, 30, 5238-5247

### Distance Distributions and Anisotropy Decays of Troponin C and Its Complex with Troponin I<sup>1</sup>

Herbert C. Cheung,<sup>1,2</sup> Chien-Kao Wang,<sup>1,3</sup> Ignacy Gryczynski,<sup>1</sup> Wieslaw Wicak,<sup>1</sup> Gabor Lacsko,<sup>1</sup> Michael L. Johnson,<sup>1</sup> and Joseph R. Lakowicz<sup>1</sup>

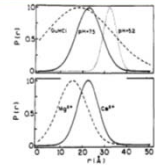
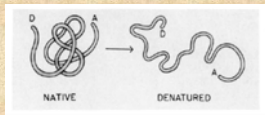


FIGURE 4: Distance distributions for Troponin C-DN2-IAE in the absence of cations (top) and in the presence of  $Mg^{2+}$  and  $Ca^{2+}$  (pH 7.5, bottom). The pH for guanidine hydrochloride (GuHCl) was 7.5.

An impressive example of the use of FRET methodologies to study protein systems is given by the work of Lillo et al. ("Design and characterization of a multisite fluorescence energy-transfer system for protein folding studies: a steady-state and time-resolved study of yeast phosphoglycerate kinase" Biochemistry. 1997 Sep 16;36(37):11261-72 and "Real-time measurement of multiple intramolecular distances during protein folding reactions: a multisite stopped-flow fluorescence energy-transfer study of yeast phosphoglycerate kinase" Biochemistry. 1997 Sep 16;36(37):11273-81)

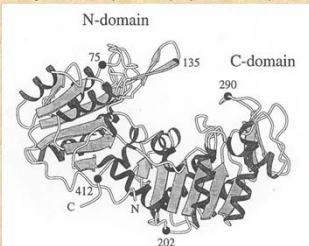
Site-directed mutagenesis was used to introduce pairs of cysteine residues in the protein at the positions shown

The pairs studied were:

135 - 290; 75 - 290

290 - 412; 412 - 202

135 - 412; 412 - 75





The donor was IAEDANS and the acceptor was IAF (iodoacetamido-fluorescein). The various labeled protein products were separated by chromatography!

Table 1: Summary of the Labeled Proteins Examined for the Photophysical Characterization of Each Energy-Transfer Pair Cys $\leftrightarrow$ Cys/

sample	name	Cys $\leftrightarrow$ Cys/	no. of cysteines	fluorophore
donor only (D-PGK)	<i>i</i> -single cysteine	D $\leftrightarrow$ -	1 (i)	AEDANS (i)
	<i>j</i> -single cysteine	- $\leftrightarrow$ D	1 (j)	AEDANS (j)
	<i>i</i> -two cysteines	D $\leftrightarrow$ -Cys	2 (i,j)	AEDANS (i)
	<i>j</i> -two cysteines	Cys $\leftrightarrow$ D	2 (i,j)	AEDANS (j)
	( <i>i,j</i> )-two cysteine average	D $\leftrightarrow$ -Cys + Cys $\leftrightarrow$ D	2 (i,j)	AEDANS (i) + AEDANS (j)
acceptor only	( <i>i,j</i> )-two cysteine "double donor"	D $\leftrightarrow$ -D	2 (i,j)	AEDANS (i,j)
	<i>i</i> -single cysteine	A $\leftrightarrow$ -	1 (i)	AF (i)
	<i>j</i> -single cysteine	- $\leftrightarrow$ A	1 (j)	AF (j)
donor-acceptor (D-PGK-A)	<i>i,j</i> specific label	D $\leftrightarrow$ A	2 (i,j)	AEDANS (i) and AF (j)
	<i>i,j</i> specific label	A $\leftrightarrow$ D	2 (i,j)	AEDANS (j) and AF (i)
	<i>i,j</i> average label	D $\leftrightarrow$ A + A $\leftrightarrow$ D	2 (i,j)	AEDANS (i) and AF (j) and + AEDANS (j) and AF (i)

Table 5: Comparison of the Measured FRET Distances with That Predicted from the Crystal Structure<sup>a</sup>

energy-transfer pair	measured steady-state distance (Å)	measured time-resolved discrete distance		measured time-resolved distance distribution				crystal structure C <sub>1</sub> -C <sub>2</sub> (Å) <sup>b</sup>	estimated dye-to-dye distance (Å) <sup>c</sup>
		R (Å)	$\chi^2$	R <sub>1</sub> (Å)	$\sigma$ (Å)	$\chi^2$	$\chi^2$		
135 $\leftrightarrow$ 290	43	43.3	2.7	39.4	7.3	1.3	39	39	
135 $\leftrightarrow$ 412	40	40.3 <sup>d</sup>	1.6	39.8 <sup>d</sup>	6.1	1.2	40	40	
412 $\leftrightarrow$ 135	40	39.5	2.7	39.5	3.8	1.3	40	40	
290 $\leftrightarrow$ 412	69	38.7	1.4	38.3 <sup>d</sup>	3.4	1.3	48	56	
75 $\leftrightarrow$ 290	56	56.6 <sup>d</sup>	1.8	58.6 <sup>d</sup>	13.2	1.4	40	46	
202 $\leftrightarrow$ 412	39	41.7	1.5	37.8	6.6	1.1	26	34	
412 $\leftrightarrow$ 75	47	46.3	1.1	46.4	5.5	1.4	32	40	
40 <sup>e</sup> $\leftrightarrow$ 75		60-70	1.1	60-80	15-30	1.1			

<sup>a</sup> Watson et al. (1982). <sup>b</sup> Donor-to-acceptor distance from MD simulations based on Watson et al. (1982) crystal structure. <sup>c</sup> Acceptor-site FRET measurements. <sup>d</sup> Unlabeled samples (MDPS buffer at pH 7.5 and 25 °C and 2 M GdCl<sub>3</sub> + MDPS buffer at pH 7.5 and 25 °C; D $\leftrightarrow$ A). <sup>e</sup> Average labeled samples (donor distributed between the two Cys sites). D $\leftrightarrow$ A: specific labeled samples. Unless otherwise indicated, distance determinations are from donor-side experiments. The errors on the recovered distances are dominated by "bleeding" sources and are estimated to be  $\pm 3$  Å (see the text).

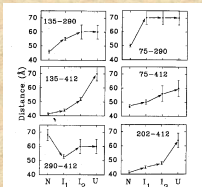
Lifetime measurements were carried out on all samples

The intramolecular distances for the six energy transfer pairs are recovered for the each intermediate formed during the GuHCL induced unfolding of PGK

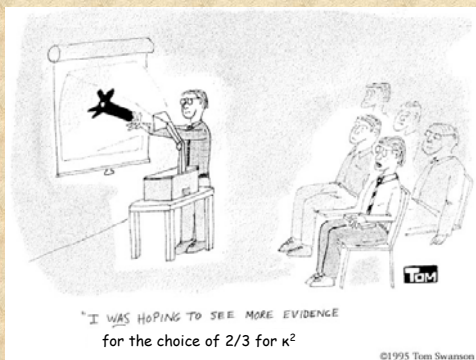
The authors proposed a specific structural transition associated with the unfolding of PGK from the native state (left) to the first unfolded state (right).



The C terminal domain (on the right of the monomer) is twisted by approximately 90° relative to the N-terminal domain resulting in an increase in the distances A,E and F and a shortening of the distance D.



The orientation factor  $\kappa^2$

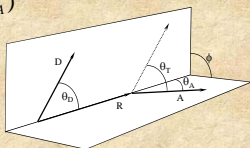


©1995 Tom Swanson

### The orientation factor $\kappa^2$

$$\kappa^2 = (\cos \theta_T - 3 \cos \theta_D \cos \theta_A)^2$$

Where  $\theta_T$  is the angle between the D and A moments, given by



$$\cos \theta_T = \sin \theta_D \sin \theta_A \cos \phi + \cos \theta_D \cos \theta_A$$

In which  $\theta_D$ ,  $\theta_A$  are the angles between the separation vector R, and the D and A moment, respectively, and  $\phi$  is the azimuth between the planes (D,R) and (A,R)

---

---

---

---

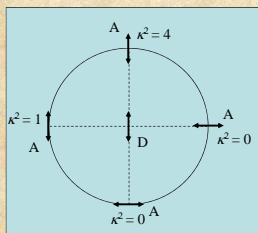
---

---

---

---

### The orientation factor $\kappa^2$



The limits for  $\kappa^2$  are 0 to 4, The value of 4 is only obtained when both transitions moments are in line with the vector R. The value of 0 can be achieved in many different ways.

If the molecules undergo fast isotropic motions (dynamic averaging) then  $\kappa^2 = 2/3$

---

---

---

---

---

---

---

---

From Eisinger and Dale in: "Excited States of Biological Molecules" Edited by John Birks (1976)

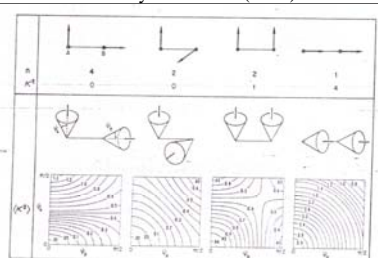


Figure 1 The upper part of the diagram illustrates the nine possible relative orientations of two transition dipoles each of which is fixed and can lie along either the x, y or z axis of a Cartesian triad. The corresponding  $\kappa^2$  values are shown along with their statistical weights (n) and they are seen to lead to an average for  $\kappa^2$  of 2/3, the same as for isotropically random orientations of the transition dipole moments. The lower part of the figure illustrates how these  $\kappa^2$  values change as the transition dipole directions are permitted orientational freedom within cones of half-angles  $\theta_D$  and  $\theta_A$ . Note that  $\langle \kappa^2 \rangle$  departs quite slowly from its fluid minimum and maximum values 0 and 4 as the two cones open up and that when each cone half-angle is  $\pi/2$ , corresponding to an isotropic distribution of the transition dipole directions,  $\langle \kappa^2 \rangle$  is equal to 2/3 for each of the cases considered.

---

---

---

---

---

---

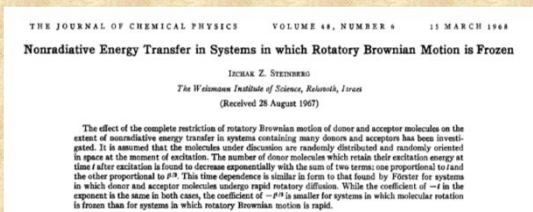
---

---

What if the system is static but randomly oriented?

For example for a system in a highly viscous solvent or in general if the fluorescence lifetimes are very short relative to any rotational motion.

Then  $\kappa^2 = 0.476$



But don't ask me to prove it!



So how do we determine  $\kappa^2$ ?

Except in very rare cases,  $\kappa^2$  can not be uniquely determined in solution.

What value of  $\kappa^2$  should be used ?

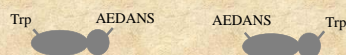
We can **assume** fast isotropic motions of the probes and value of  $\kappa^2 = 2/3$ , and verify experimentally that it is indeed the case.

We can **calculate** the lower and upper limit of  $\kappa^2$  using polarization spectroscopy (Dale, Eisinger and Blumberg 1979).

Assuming  $\kappa^2 = 2/3$

We can test this assumption experimentally:

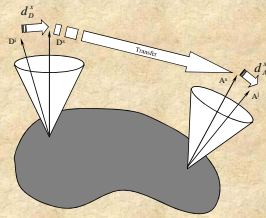
**By swapping probes:** The micro-environment of the probes will be different. Therefore, if the micro-environment affect the probes mobility and,  $\kappa^2$  is not equal to  $2/3$ , once swapped, the value of  $\kappa^2$  will changed and hence the distance measured by FRET.



**By using different probes:** If the distance measured using different probe pairs are similar (taking into account the size of the probes) then the assumption that  $\kappa^2$  is equal to  $2/3$  is probably valid.

## Lower and upper limit of $\kappa^2$

We can calculate the lower and upper limit of  $\kappa^2$  using polarization (Dale, Eisinger and Blumberg 1979).



Lets consider that the each probe are rotating within a cone of axes  $D^*$  and  $A^*$  for the donor and acceptor, respectively, then 3 depolarization steps occurs after the absorption of the excitation energy by the donor: An axial depolarization of the donor, a depolarization due to transfer and an axial depolarization of the acceptor

In the Dale-Eisinger-Blumberg approach, one measures the ratio of the observed polarizations of donors and acceptors to their limiting polarizations and then uses the calculated contour plots to put limits on  $\kappa^2$

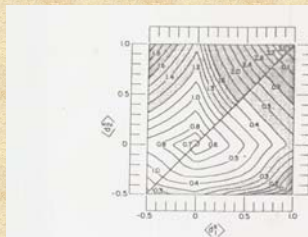


FIGURE 9. Contour plot similar to those shown in Figs. 4-8, but applicable in situations in which  $\langle \cos^2 \theta \rangle$ , and hence  $P_0$ , is unknown. It is obtained by maximizing and minimizing Eq. 21 and can be used to lead to larger ranges between  $\langle \cos^2 \theta \rangle_{\text{max}}$  and  $\langle \cos^2 \theta \rangle_{\text{min}}$  than the plots of Figs. 4-8. In the lightly stippled regions the error in  $R$  resulting from the use of  $\langle \cos^2 \theta \rangle = 0$  instead of the indicated  $\langle \cos^2 \theta \rangle_{\text{max}}$  and  $\langle \cos^2 \theta \rangle_{\text{min}}$  is greater than 20%. It is between 10% and 20% in the lightly stippled regions and less than 10% in the unshaded areas.

This approach was used in:

Arbildua et al.,

*Fluorescence resonance energy transfer and molecular modeling studies on 4',6-diamidino-2-phenylindole (DAPI) complexes with tubulin.*

Protein Sci. (2006) 15(3):410-9.

FRET occurs between DAPI and TNP-GTP bound to tubulin – a heterodimer protein

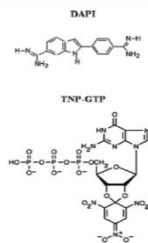


Figure 1. Structures of 4',6-diamidino-2-phenylindole (DAPI) and 7,7'-O-(2,4,6-trinitrocyclohexadienylidene)-GTP (TNP-GTP) at neutral or basic pH.

Assuming a  $\kappa^2$  value of 2/3, one would calculate the DAPI-TNP-GTP distance to be ~43 Angstroms

But DAPI is bound non-covalently - hence has no local motion so its polarization is high (~0.42)

And, TNP-GTP is also non-covalently bound and has a short lifetime and hence a high polarization (~0.48)

These observed polarization values are close to the limiting polarization values for these probes: 93% and 100% respectively, for DAPI and TNP-GTP

---

---

---

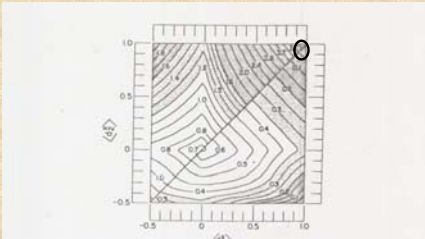
---

---

---

---

Using the Dale-Eisenger-Blumberg plot one can then estimate that  $\kappa^2$  can be anywhere between 0.02 and 3.7!



In fact the authors concluded, based on other information, that the distance between DAPI and TNP-GTP bound to tubulin was likely to ~ 30 Angstroms.

---

---

---

---

---

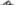
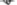


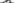
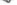

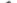
---

---

**Energy Transfer in tRNA<sup>Pro</sup> (Yeast). The Solution Structure of Transfer RNA**

W. E. BLUMBERG, R. E. DALE,\* J. EISINGER, and  
D. M. ZÜCKERMAN, *Bell Laboratories, Inc.,  
Murray Hill, New Jersey 07874*

**TABLE II**  
Maximum and Minimum Values of the Orientation Factor and Ratio of Derived Separation  $R$  to that Obtained Using the Dynamic Random Average (Isotropic) Value  $R_{1/2}$

Model <sup>a</sup>	Figure <sup>a</sup>	Y-A	$\langle \kappa^2 \rangle$	R/R <sub>1/2</sub>	
4(1)	cc	10		3.13 ± 0.08	1.29 ± 0.01
	cC	11		3.13 ± 0.08	1.29 ± 0.01
	Cc	11		3.13 ± 0.08	1.29 ± 0.01
	CC	12		3.13 ± 0.08	1.29 ± 0.01
4(2)	cc	13		0.115 ± 0.012	0.75 ± 0.01
	cC	14		0.115 ± 0.012	0.75 ± 0.01
	Cc	14		0.115 ± 0.012	0.75 ± 0.01
	CC	15		0.115 ± 0.012	0.75 ± 0.01

---

---

---

---

---

---

---



Assuming an average value of 2/3 for  $\kappa^2$ , Beardsley and Cantor<sup>2</sup> estimated the separation between the Y base adjacent to the anticodon and acriflavine bound at the CCA terminus of tRNA<sup>Phe</sup> (yeast) to be about 46 Å. The analysis presented here indicates a possible range of 34–61 Å at the most.

A 3D ribbon diagram of a DNA double helix. The two strands are colored blue and red. A red arrow points from the top of the helix to the bottom, with the text  $\sim 77\text{\AA}$  next to it.

But FRET can be very powerful when used to detect changes in a system, such as alterations in distance and/or orientation between donor and acceptor attached to biomolecules, i.e., due to ligand binding or protein-protein interactions

## nature structural biology • volume 7 number 9 • september 2000

[illegible]

Nathan Sanner, Lei Wang, Paul Steinboeck



## Homo-transfer of electronic excitation energy

So far, we considered the donor and acceptor molecules to be different. However, if the probe excitation spectrum overlaps its emission spectrum, FRET can occur between identical molecules.

« Il suffit qu'un transfert d'activation puisse se produire entre deux molécules voisines d'orientation différentes, c'est à dire portant des oscillateurs non parallèles, pour qu'il en résulte en moyenne une diminution de l'anisotropie de distribution des oscillateurs excités et par suite de la polarisation de la lumière émise. »

(F. Perrin *Ann de Phys.* 1929)

It suffices that a transfer of activation can occur between two neighboring molecules with different orientations, that is with non-parallel oscillators, in order to have, on average, a decrease in the anisotropy of the distribution of excited oscillators, and therefore a decrease of the polarization of the emitted light.

« ...L'existence de transferts d'activation est expérimentalement prouvée pour de telles molécules par la décroissance de la polarisation de la lumière de fluorescence quand la concentration croît... »

(F. Perrin *Ann de Phys.* 1932)

...The existence of transfer of activation is proven experimentally for such molecules by the decrease in polarization of the fluorescent light when the concentration is increased...

---

---

---

---

---

---

---

---

Electronic energy transfer between identical fluorophores was originally observed by Gaviola and Pringsheim in 1924.

### Über den Einfluß der Konzentration auf die Polarisation der Fluoreszenz von Farbstofflösungen.

Von E. Gaviola und Peter Pringsheim in Berlin.

Mit zwei Abbildungen. (Eingegangen am 24. März 1924.)

Tabelle 2. Uranin in ganz wasserfreiem Glycerin.

$C$	$p$	$C$	$p$	$C$	$p$	$C$	$p$
$\frac{1}{4}$	0	$\frac{1}{32}$	6,5	$\frac{1}{256}$	15	$\frac{1}{2048}$	39,2
$\frac{1}{8}$	?	$\frac{1}{64}$	8,1	$\frac{1}{512}$	19,5	$\frac{1}{4100}$	48,5
$\frac{1}{16}$	3,2	$\frac{1}{128}$	11,1	$\frac{1}{1024}$	30,7	etwa $\frac{1}{20000}$	45

(note: uranin is the sodium salt of fluorescein)

---

---

---

---

---

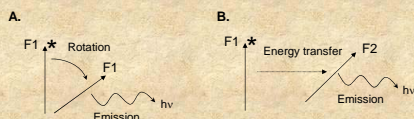
---

---

---

## Homo-transfer of electronic excitation energy

"...Excitation transfer between alike molecules can occur in repeated steps. So the excitation may *migrate* from the absorbing molecule over a considerable number of other ones before deactivation occurs by fluorescence or other process. Though this kind of transfer cannot be recognized from fluorescence spectra, it may be observed by the decrease of fluorescence polarization..." (Förster, 1959)



**A.** Depolarization resulting from rotational diffusion of the fluorophore. The excited fluorophore ( $F1^*$ ) rotates then emits light. **B.** The excited fluorophore ( $F1^*$ ) transfer energy to another fluorophore  $F2$  which in turn emits light.

---

---

---

---

---

---

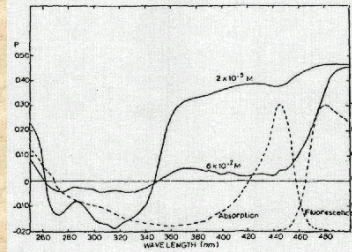
---

---

### Weber's Red-Edge Effect

In 1960 Weber was the first to report that homotransfer among indole molecules disappeared upon excitation at the red-edge of the absorption band - this phenomenon is now known as the "Weber red-edge effect".

In 1970 Weber and Shinitzky published a more detailed examination of this phenomenon. They reported that in the many aromatic residues examined, transfer is much decreased or undetectable on excitation at the red edge of the absorption spectrum.




---

---

---

---

---

---

---

---

### Distance determination using homotransfer

The efficiency of transfer can be calculated from a knowledge of the polarization in the absence and presence of energy transfer.

The steady state expression for the efficiency of energy transfer ( $E$ ) as a function of the anisotropy is given by

$$E = 2(r_d - \langle r \rangle) / (r_d - r_a)$$

Where  $r_d$  and  $r_a$  are the anisotropy decay of the donor and acceptor only, respectively and  $\langle r \rangle$  is the observed anisotropy in presence of both donor and acceptor. If  $\kappa^2 = 2/3$  then  $r_a = 0$  and

$$E = 2(r_d - \langle r \rangle) / r_d$$

---

---

---

---

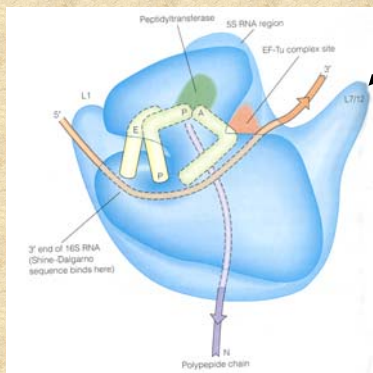
---

---

---

---

An example of homo-FRET used to study protein interactions is the work by Hamman et al (Biochemistry 35:16680) on a prokaryotic ribosomal protein




---

---

---

---

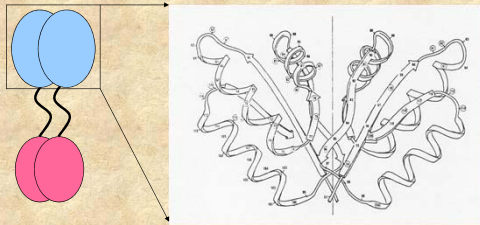
---

---

---

---

L7/L12 is present as two dimers in the ribosome. An X-ray structure of monomeric C-terminal domains led to the speculation that the C-terminal domains of L7/L12 interacted through hydrophobic surfaces as shown below




---

---

---

---

---

---

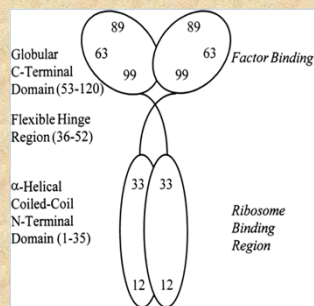
---

---

To study this protein fluorescence probes were introduced at specific locations along the L7/L12 peptide backbone.

To introduce these probes at specific locations site-directed mutagenesis was used to place cysteine residues in different locations

Sulfhydryl-reactive fluorescence probes were then covalently attached to these cysteine residues




---

---

---

---

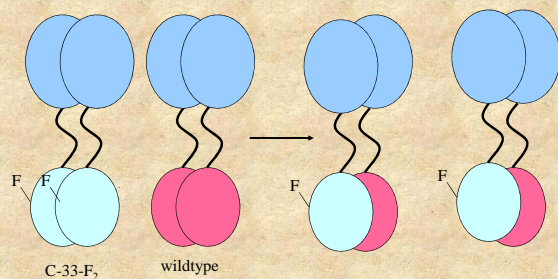
---

---

---

---

Subunit exchange experiments allowed the preparation of singly labeled dimers




---

---

---

---

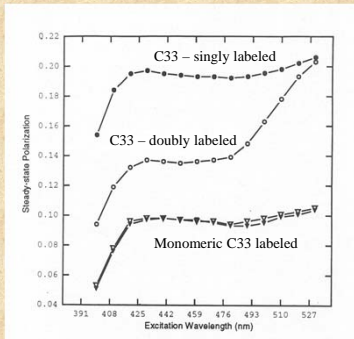
---

---

---

---

The presence of homoFRET was evident in the excitation polarization spectrum as shown by the Weber Red-Edge Effect.




---

---

---

---

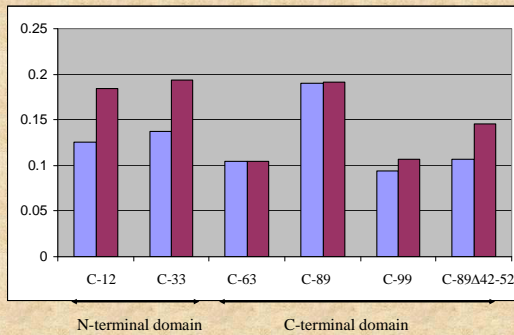
---

---

---

---

The polarization values, before and after subunit exchange, indicate which residues undergo homoFRET. The polarization data below are for fluorescein labeled constructs before (violet) and after (magenta) subunit exchange




---

---

---

---

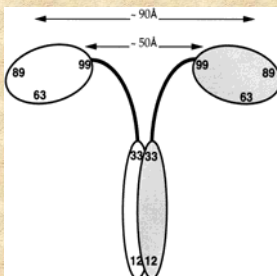
---

---

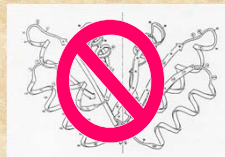
---

---

These changes in polarization due to homoFRET allow us to assign maximum proximity values for the C-terminal domains.



The conclusion is that the C-terminal domains are well-separated – contrary to the original model from the X-ray studies and the usual depictions in the literature




---

---

---

---

---

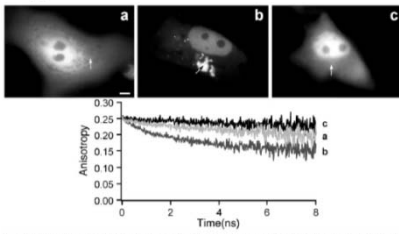
---

---

---

I. Gautier,\* M. Tramier,\* C. Durieux,\* J. Coppey,\* R. B. Pansu,<sup>†</sup> J.-C. Nicolas,<sup>‡</sup> K. Kemnitz,<sup>§</sup> and M. Coppey-Moisan\*

I. Gautier,\* M. Tramier,\* C. Durieux,\* J. Coppey,\* R. B. Pansu,<sup>†</sup> J.-C. Nicolas,<sup>‡</sup> K. Kemnitz,<sup>§</sup> and M. Coppey-Moisan\*

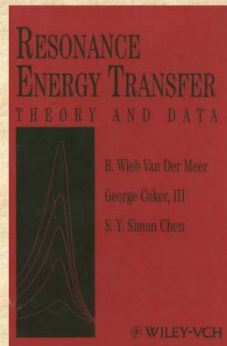


Biophys J, June 2001, p. 3000-3008, Vol. 80, No. 6

Other examples of homo-FRET *in vivo* can be found in: Tramier et al., 2003 "Homo-FRET versus hetero-FRET to probe homodimers in living cells" *Methods Enzymol.* 360:580-97.

To summarize this lecture is not intended to prepare you to start FRET measurements immediately but rather to make you aware of the salient principles and pitfalls

Several books on this topic are available as well as MANY articles in the primary literature



## Fluorescence Probes

*In vitro* (or *In Silico*)

*In vivo* (or more accurately in cells)

Many of these slides were prepared by  
Susana Sanchez  
and  
Ewald Terpetschnig

---

---

---

---

---

---

---

## Classification:

- Intrinsic Fluorophores
- Extrinsic Fluorophores

---

---

---

---

---

---

---

## Intrinsic Fluorophores

Naturally Occurring Fluorophores

---

---

---

---

---

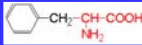
---

---

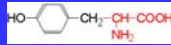


## Proteins: Naturally Occurring Fluorophores

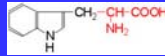
### Aromatic amino acids



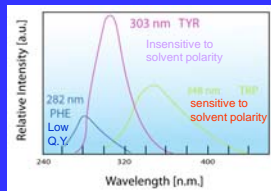
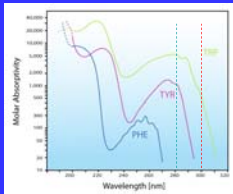
**Phenylalanine (Phe – F)**  
Ex/em 260 nm/282 nm



**Tyrosine (Tyr – Y)**  
Ex/em 280 nm/303 nm

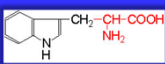


**Tryptophan (Trp-W)**  
Ex/em 280, 295nm/ 305-350 nm



## Tryptophan derivatives

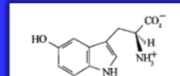
Tryptophan derivatives may be genetically incorporated in a protein



**Tryptophan**  
ex/em 280, 295nm/ 305-350 nm

$$\phi = 0.14$$

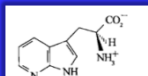
•solvent-sensitive emission



**5-Hydroxy-tryptophan**  
ex/em 310nm/339 nm

$$\phi = 0.097$$

•solvent-insensitive emission



**7-azatryptophan**  
ex/em 320nm/403nm

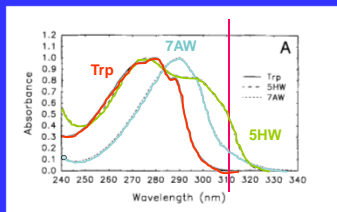
$$\phi = 0.017$$

•Large emission shift in water

$\phi$  =Number of photons emitted/number of photons absorbed

*Protein Science (1997), 6, 689-697.*

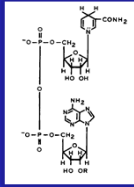
Absorbance spectrum is red-shifted with respect to that of tryptophan.



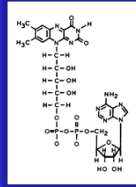
It is possible to selectively excite them, in the presence of tryptophan of other proteins

*Protein Science (1997), 6, 689-697.*

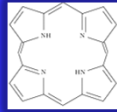
### Enzymes Cofactors



**NADH**  
(oxido-reductases)  
Ex/Em 340/460 nm



**FAD**  
(metabolic enzymes)  
(ex/em 450nm/540 nm)



**Porphyrins**  
(ex/em 550 nm/620 nm).

---

---

---

---

---

---

---

---

### Extrinsic Fluorophores

Synthetic dyes or modified biochemicals that are added to a specimen to produce fluorescence with specific spectral properties

---

---

---

---

---

---

---

---

### Fluorescent Probes:

- Non covalent interactions

A fluorescent probe is a fluorophore designed to localize within a specific region of a biological specimen or to respond to a specific analyte.

- Covalent interactions

---

---

---

---

---

---

---

---

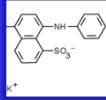
## Extrinsic probes

(not present in the natural molecule/macromolecule)

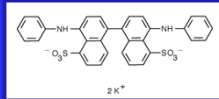
### Non-covalent Attachment

Barely fluorescent in pure water but their fluorescence can be strongly enhanced if the environment becomes hydrophobic (hydrophobic patches on proteins)

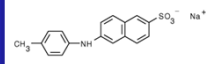
1,8-ANS



bis-ANS



2,6-TNS

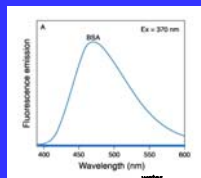
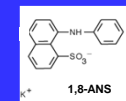


## Fluorescent Probes

*Non-covalent*

### 1,8-ANS

Developed by G. Weber in the early 1950's

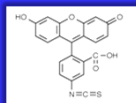


Barely fluorescent in water  
- fluorescence is strongly enhanced in hydrophobic environments

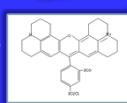
It is interesting to note that even today, more than 50 years after that first report, ANS is still being used in protein studies, quite often as an indicator of the "molten globular" state.



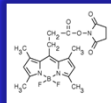
### Fluorescent groups



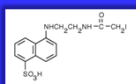
**FITC**  
(488/512)  $\tau = 4.05$



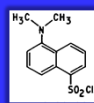
**Texas Red**  
(595-615)  $\tau = 3.5$  ns



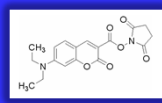
**BODIPY**  
(493/503)  $\tau = 1$  ns



**IAEDANS**  
(360/480)  $\tau = 15$  ns

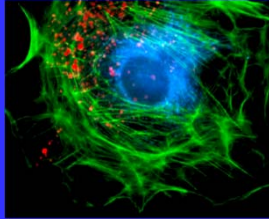


**1,5-Dansyl chloride**  
(335/518)  $\tau = 10-17$  ns



**Coumarin-3-carboxylic acid-NHS**  
(445/482)  $\tau = 2-3$  ns

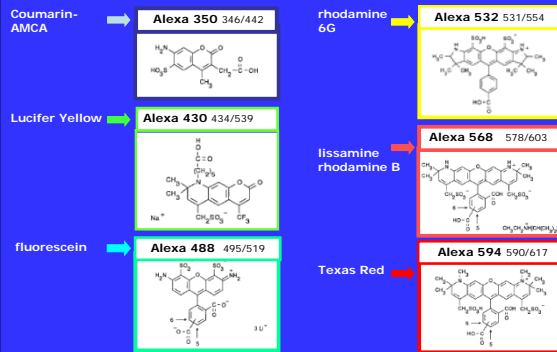
## The Alexa-Fluor series



1999  
"there is a need  
for probes with high fluorescence  
quantum yield and high  
photostability to allow detection of  
low-abundance biological  
structures with great sensitivity  
and selectivity"

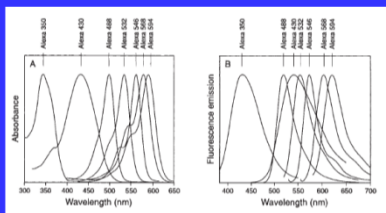
*The Journal of Histochemistry & Cytochemistry* Volume 47(9): 1179–1188, 1999. Molecular Probes, Inc., Eugene, Oregon

## Designed to be more photostable than their commonly used spectral analogues



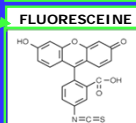
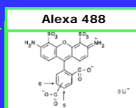
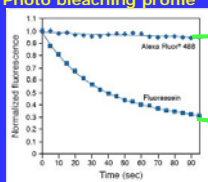
All Alexa dyes and their conjugates are more fluorescent and more photostable than their commonly used spectral analogues.

In addition, Alexa dyes are insensitive to pH in the 4–10 range.



*The Journal of Histochemistry & Cytochemistry* Volume 47(9): 1179–1188, 1999. Molecular Probes, Inc., Eugene, Oregon

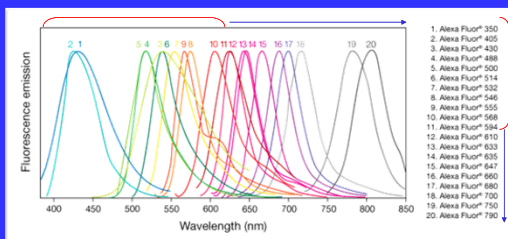
### Photo bleaching profile



- Cells stained with Alexa Fluor488 or fluorescein conjugates of goat anti-mouse IgG antibody
- Samples were continuously illuminated and images were collected every 5 seconds with a cooled CCD camera.

<http://www.invitrogen.com/>

## The Alexa series expanded



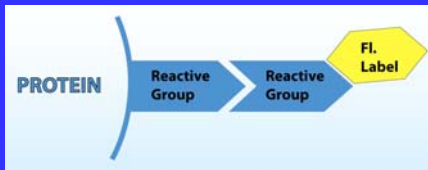
Alexa Fluor dyes are available as amine-reactive succinimidyl esters

Fluorescence quantum yields (QY) and lifetimes ( $\tau$ ) for Alexa Fluor dyes–

Alexa Fluor Dye *	QY †	$\tau$ (ns) ‡
Alexa Fluor 488	0.92	4.1 §
Alexa Fluor 532	0.61	2.5
Alexa Fluor 546	0.79	4.1
Alexa Fluor 555	0.10	0.3
Alexa Fluor 568	0.69	3.6 §
Alexa Fluor 594	0.66	3.9 §
Alexa Fluor 647	0.33	1.0
Alexa Fluor 660	0.37	1.2 **
Alexa Fluor 680	0.36	1.2
Alexa Fluor 700	0.25	1.0
Alexa Fluor 750	0.12	0.7

<http://www.invitrogen.com>

## Protein Labeling



Reactive groups on proteins

**NH<sub>2</sub>** Lysine  
N-terminus

**SH** Cysteine

Depends on the reactive group on the protein

Light source

Spectral properties

Autofluorescence

Photostability

Labeling should not alter the biological activity of biomolecules

---

---

---

---

---

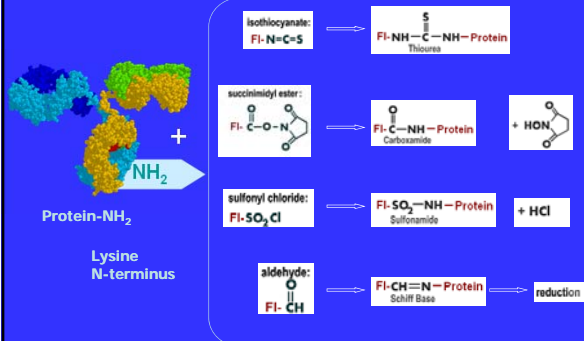
---

---

---

## Protein Labeling

### Amino-Modification:




---

---

---

---

---

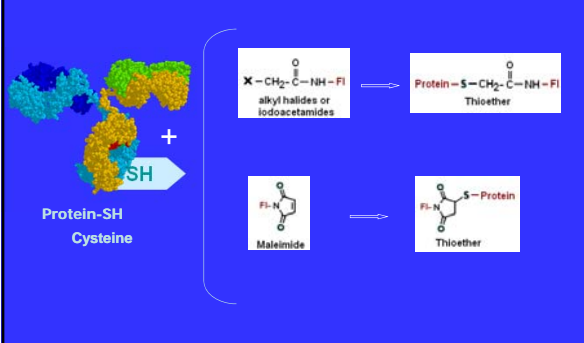
---

---

---

## Protein Labeling

### Thiol-Modification:




---

---

---

---

---

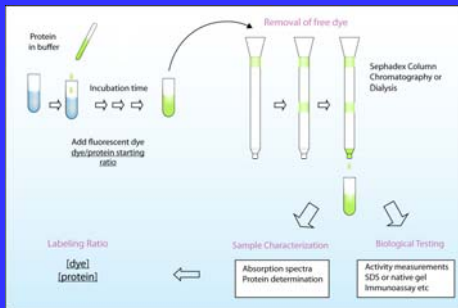
---

---

---



## Labeling Procedure




---

---

---

---

---

---

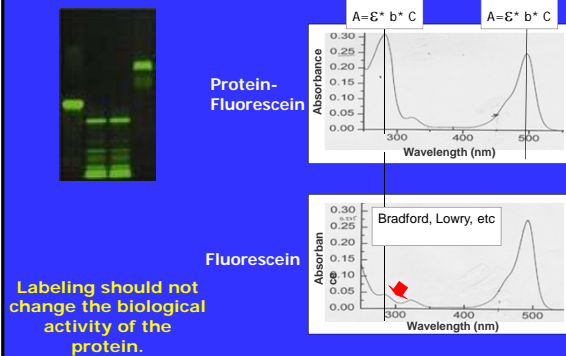
---

---

---

---

## Characterization after the labeling




---

---

---

---

---

---

---

---

---

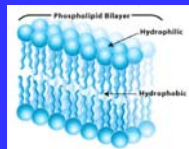
---

## Labeling membranes

- Analogs of fatty acids and phospholipids

- Di-alkyl-carbocyanine and Di-alkyl-aminostyryl probes.

- Other nonpolar and amphiphilic probes.  
DPH, Laurdan, Prodan, Bis ANS




---

---

---

---

---

---

---

---

---

---

# Membrane Probes

## Microviscosity and Order in the Hydrocarbon Region of Micelles and Membranes Determined with Fluorescent Probes. I. Synthetic Micelles\*

M. Winkler, J. A.C. Drenth, J. C. Gille, and G. Weber

Abstract: The viscosity in micelle interiors, termed here as microviscosity, was derived from an analysis comparing the degree of fluorescence depolarization of pyrene or 2-methylanthracene when dissolved in the tested micelles and in American white oil (C<sub>10</sub> H<sub>18</sub>). The latter was used as a reference solvent of known viscosity. In the series studied, hexamethylphosphoramide, triethylamine, methoxybenzylamine, methoxybenzylamine, and methoxybenzylamine (CTAB), and methoxybenzylamine (CTAB) were used. The microviscosity at 27 °C was all in the range of 17–50 cP. The change in microviscosity with temperature in the series was found to follow a single exponential law with an activation energy in the range of 41–54 kJ mol<sup>-1</sup>. Added salts affected only slightly the microviscosity values, except micelles of pyrene-labeled CTAB with vinyl alcohol or cholesterol

and with sodium laurylsulfate. These results were used to test the effect of shape, volume and charge concentration on the fluidity of the micelle interior. The microviscosity of these micelles was found to increase mainly with concentration of the solvent component, and in a smaller rate also with the microviscosity of the solvent. The change in apparent viscosity of the micelles with temperature indicates that the depolarizing motions are more or less hindered. The microviscosity in pyrene is not related to the micelle phase transition, independently of the medium studied, pyrene in glycerol at -147 °C, pyrene in glycerol at -1 °C. This indicates that the viscosity in the micelle is the same as in the bulk. A summary of the micelle properties and the microviscosity data is given.

In general, the fluorescence emitted from molecules which are dissolved in a viscous medium is partially polarized. This is commonly explained in terms of molecular orientation, i.e., in terms of polarization, which is measured as right angle to polarization extinction ratio and is defined as

$$r = \frac{I_{\parallel} - I_{\perp}}{I_{\parallel} + 2I_{\perp}} \quad \rho = \frac{I_{\parallel} - I_{\perp}}{I_{\parallel} + I_{\perp}} \quad (1)$$

\* From the Department of Chemistry, School of Chemical Sciences, University of Illinois, Urbana, Illinois 61801. Present address: J. C. Gille, 1000 S. 1st St., St. Louis, MO 63102. G. Weber, 1000 S. 1st St., St. Louis, MO 63102. M. Winkler, 1000 S. 1st St., St. Louis, MO 63102. J. A.C. Drenth, 1000 S. 1st St., St. Louis, MO 63102.

2106 JOURNAL OF POLYMER SCIENCE, VOL. 15, NO. 11, 1971

When  $I_{\parallel}$  and  $I_{\perp}$  are the fluorescence intensities observed through a polarizer oriented parallel and perpendicular to the plane of polarization of the excitation beam. For a rotating fluorescent sphere the observed  $r$  or  $\rho$  values after the well known factor (1/2) correction to which  $I_{\parallel}$  and  $I_{\perp}$  are the values

$$r = \frac{1}{2} \left( \frac{I_{\parallel} - I_{\perp}}{I_{\parallel} + I_{\perp}} \right) \quad \rho = \frac{1}{2} \left( \frac{I_{\parallel} - I_{\perp}}{I_{\parallel} + I_{\perp}} \right) \quad (2)$$

of  $r$  and  $\rho$  when the emitting molecules maintain their orientation relative to the plane of polarization of the excitation beam.  $\rho$  is the ratio of intensities of the plane and  $r$  is the ratio of fluorescence intensities. The term  $r$  is defined here in the diagram of fluorescence.

## Dynamics of the Hydrocarbon Layer in Liposomes of Lecithin and Sphingomyelin Containing Diethylphosphite\*

MAURICE BERNHART AND YOUNGJAE BARNHART

From the Department of Biophysics, The Weizmann Institute of Science, Rehovot, Israel, and the Department of Biochemistry, The Hebrew University, Jerusalem, Israel

(Received for publication, September 12, 1970)

### SUMMARY

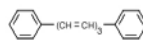
Physical properties of the hydrocarbon region in lipid bilayers were studied in a series of liposomes of lecithin and sphingomyelin, containing different concentrations of diethylphosphite. The bilayers were studied by fluorescence polarization and by fluorescence polarization analysis of a specific probe embedded in the hydrocarbon region. The two probes employed in this study were pyrene and 1,6-diphenyl-1,3,5-triazine, which undergo a strong fluorescence quenching and a strong fluorescence enhancement, respectively. The determined dynamic properties of the hydrocarbon region in the bilayers liposomes differ markedly from those of the sphingomyelin liposomes. The hydrocarbon region of the lecithin liposomes is of an isotropic phase between 0° and 40° characterized by a microviscosity of 25 cP, a Q<sub>11</sub> of 0.4, a Q<sub>22</sub> of 0.1, and a kinetic activation energy, E<sub>a</sub>, of 8 ± 4 kJ per mole. In contrast to lecithin, the hydrocarbon region of the sphingomyelin liposomes displays a distinct phase transition at 17 ± 1°. The phase at low temperatures, where the transition point, presumably a lipid crystalline phase, is characterized by E<sub>a</sub> = 18 ± 4 kJ per mole, whereas the phase below is, presumably a gel state, possesses a E<sub>a</sub> value lower than 1 kJ per mole. In addition to that, the hydrocarbon region in sphingomyelin liposomes is much more viscous than in lecithin liposomes as shown by E<sub>a</sub> = 25 ± 4 kJ per mole. All of these observations are only slightly and irregularly affected by the presence of diethylphosphite, despite the strong effects it exerts on the surface energy potential of the liposomes. The observation that the forces which dictate the dynamic properties of the hydrocarbon region in lipid bilayers predominantly originate from hydrophobic interactions.

different and specific value for each transition region. In some membranes this value changes drastically with age (3, 4). The molecular structure of sphingomyelin and lecithin can be separated into two distinct regions: the hydrophilic region, which contains the phosphate groups in both heads, and the hydrophobic region, which contains the hydrocarbon chains. In addition to the hydrocarbon chains, the ester groups of lecithin contain two other heads, whereas that of sphingomyelin contains an amide bond, an hydroxyl group, and a base-labile head. These groups result in differences in the net dipole moment and in the ability to form hydrogen bonds (5, 6). In the hydrophilic region the average length of the hydrocarbon chains is higher in sphingomyelin than in lecithin, and the degree of conformation is greater than in sphingomyelin (7). The general nature of these groups affects the structure and dynamics of lipid bilayers. In this study, structure and dynamic properties of oriented bilayers, made of sphingomyelin or lecithin containing diethylphosphite, were investigated. The method employed was fluorescence polarization (8, 9) and is based on measurement of fluorescence polarization of a hydrocarbon probe and recording in the microviscosity,  $\eta$ , which is related to the kinetic energy of the probe (e.g., probe). From the temperature profile of  $\eta$  phase transitions were detected and the transition enthalpies,  $\Delta H$ , of each phase were determined (5, 6).

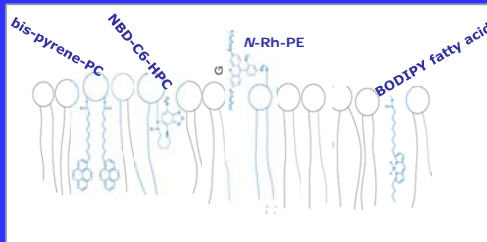
### EXPERIMENTAL PROCEDURES

Phospholipid-liposomes were prepared from egg yolk (10) and purified chromatographically on alumina and silica columns (11). The vesicles were then washed with distilled water and the water was removed and lyophilized with phosphorus. The vesicles were then washed with a Packed gel column chromatography on 10% ethylene glycol methacrylate columns. The obtained

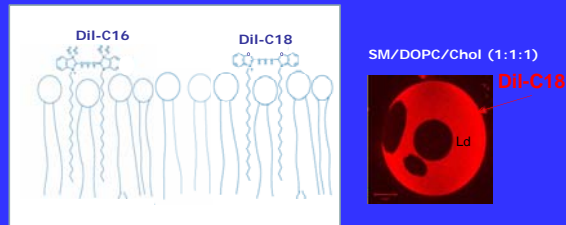
## DPH - diphenylhexatriene



# Fatty acids analogs and phospholipids



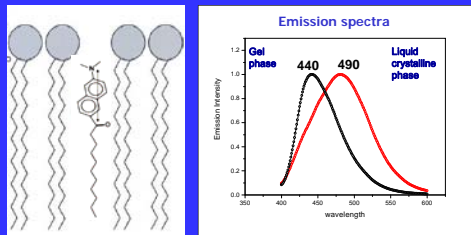
## Di-alkyl-carbocyanine probes.



*Chem. and Phys. of Lipids* 141 (2006) 158–168

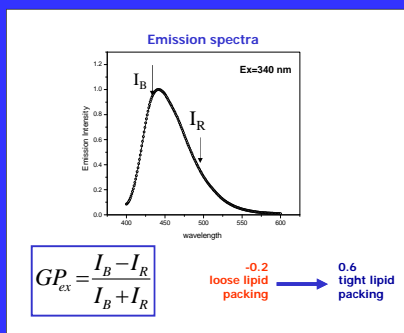
## Nonpolar probes

example: *Laurdan*  
(environment-sensitive spectral shifts)



Weber, G. and Farris, F. *J. Biochemistry*, 18, 3075-3078 (1979).

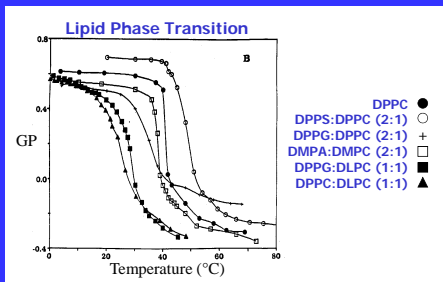
## Laurdan Generalized Polarization (GP)



*Parasassi et al. Biophysical J.*, 60, 179-189 (1991).

## GP in the cuvette

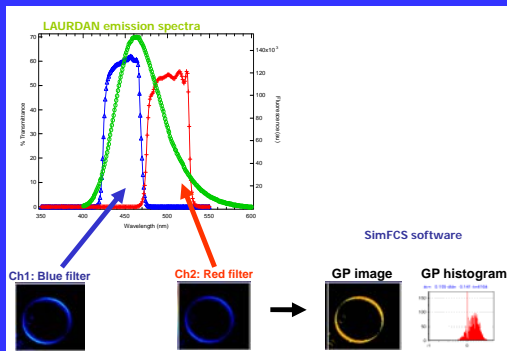
MLVs, SUVs, LUVs



Parassassi et al. Biophys. J. 60, 179 (1991)

## GP in the microscope

(2-photon excitation)



## Fluorescent Ion-Probes

Fluorescence probes have been developed for a wide range of ions:

### Cations:

H<sup>+</sup>, Ca<sup>2+</sup>, Li<sup>+</sup>, Na<sup>+</sup>, K<sup>+</sup>, Mg<sup>2+</sup>, Zn<sup>2+</sup>, Pb<sup>2+</sup> and others

### Anions:

Cl<sup>-</sup>, PO<sub>4</sub><sup>2-</sup>, Citrate, ATP, and others

## Probes For Calcium determination

### UV

#### FURA

(Fura-2, Fura-4F, Fura-5F, Fura-6F, Fura-FF)

#### INDO

(Indo-1, Indo 5F)

**Ratiometric**

### VISIBLE

#### FLUO

(Fluo-3, Fluo-4, Fluo5F, Fluo-5N, Fluo-4N)

**RHOD** ( Rhod-2, Rhod-FF, Rhod-5N)

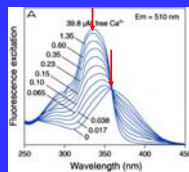
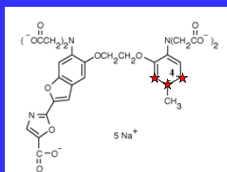
**CALCIUM GREEN** (CG-1, CG-5N,CG-2)

**OREGON GREEN 488-BAPTA**

**Non  
Ratiometric**

## Ratiometric: 2 excitation/1emission

### FURA-2



Indicator	$K_d$ ( $\text{Ca}^{2+}$ )
Fura-2	0.14 $\mu\text{M}$
Fura-5F	0.40 $\mu\text{M}$
Fura-4F	0.77 $\mu\text{M}$
Fura-6F	5.30 $\mu\text{M}$
Fura-FF (5,6)	35 $\mu\text{M}$

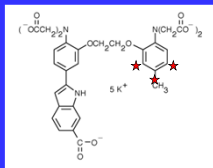
Most used in microscopic imaging

Good excitation shift with  $\text{Ca}^{2+}$

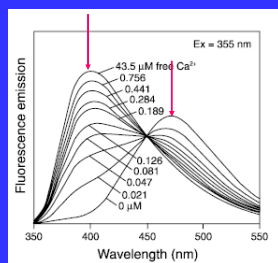
Rationed between 340/350 and 380/385 nm

## Ratiometric: 1excitation /2emission

### Indo-1

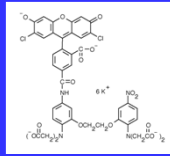


Indicator	$K_d$ ( $\text{Ca}^{2+}$ )
Indo-1	0.23
Indo-5F	0.47

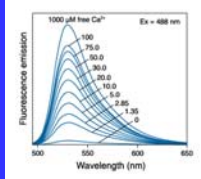


## CalciumGreen-5N

Non-Ratiometric

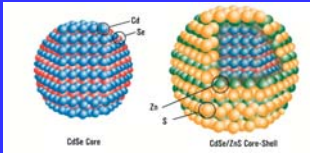


Fluorescence Intensity





Quantum Dots



---

---

---

---

---

---

---

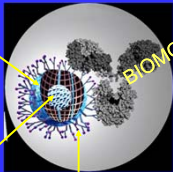
---

Quantum Dots

Nanometer-Scale Atom Clusters

**CORE**  
Cadmium selenide (CdSe), or  
Cadmium telluride (CdTe)  
few hundred – few thousand atoms

The semiconductor material is chosen  
based upon the emission wavelength,  
however it is the size of the particles  
that tunes the emission  
wavelength.



**SHELL**  
In the core emission is typically weak  
and always unstable.  
The shell material (ZnS) has been  
selected to be almost entirely  
unreactive and completely insulating  
for the core.

**COATING**  
A layer of organic ligands covalently attached to the surface  
of the shell. This coating provides a **surface for  
conjugation** to biological (antibodies, streptavidin, lectins,  
nucleic acids) and nonbiological species and makes them  
water-soluble.

---

---

---

---

---

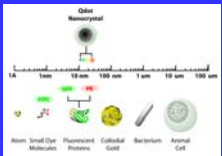
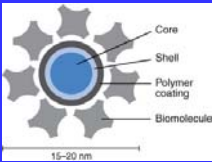
---

---

---

Quantum Dots

Nanometer-Scale Atom Clusters



Quantum Dot Material System	Emission Range	Quantum Dot Diameter Range	Quantum Dot Type	Standard Solvents	Example Applications
CdSe	465nm - 640nm	1.9nm - 6.7nm	Core	Toluene	Research, Solar Cells, LEDs
CdSe/ZnS	490nm - 620nm	2.9nm - 6.1nm	Core-Shell	Toluene	Visible Fluorescence Applications, Electroluminescence, LEDs
CdTe/CdS	620nm - 680nm	3.7nm - 4.8nm	Core-Shell	Toluene	Deep Red Fluorescence Apps.

---

---

---

---

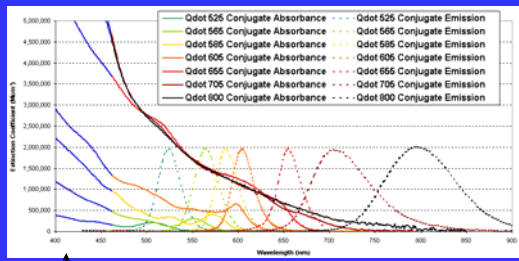
---

---

---

---

## Qdot Optical Spectra



Violet excitation

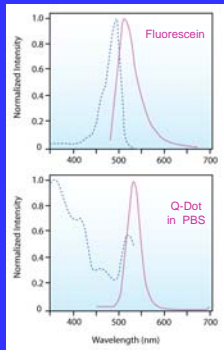
Absorbance  $\times$  Quantum Yield = Brightness  
 photons in      fraction converted      photons out

Broad range of emissions

High absorbance means increased brightness  
 Single-color excitation, multicolor emission for easy multiplexing

Courtesy of Invitrogen

## Qdot Summary



### Advantages:

Broad absorption spectra, making it possible to excite all colors of QDs simultaneously with a single light source - **Multiplexing**

Narrow and symmetrical emission spectra

**Emission tunable** with size and material composition

Exhibit excellent **photo-stability**

### Disadvantages:

**Large size and high mass** limit their use in applications requiring high diffusional mobility

QDot	$\lambda_{exc}$ (nm)	$\lambda_{em}$ (nm)	$\epsilon$ (M <sup>-1</sup> cm <sup>-1</sup> )	Q.Y.
655	350	655	9,000,000	~0.5
705	350	705	13,000,000	~0.5
800	350	800	13,000,000	~0.5

## The Fluorescent Toolbox for Assessing Protein Location and Function

Ben N. G. Geopman,<sup>1,2</sup> Stephen R. Adams,<sup>1</sup> Mark H. Ellman,<sup>1</sup> Roger Y. Tsien<sup>1,2\*</sup>  
 SCIENCE VOL 312 14 APRIL 2006

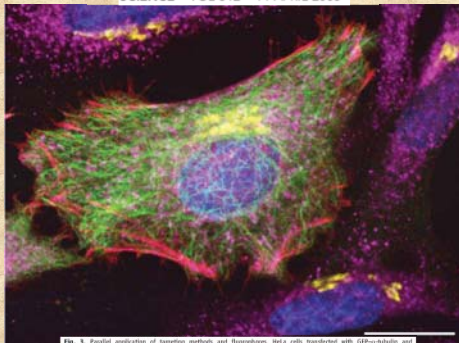
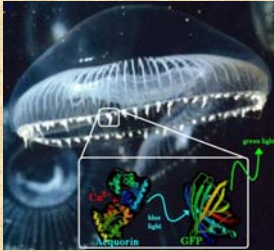
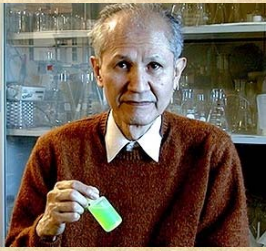


Fig. 3. Parallel application of targeting methods and fluorescent dyes. HeLa cells transfected with GFP-actin and mCherry-myc were stained with Hoechst. After fixation, cells were immunolabeled for the Golgi matrix protein giantin with QDs and for the mitochondrial enzyme cytochrome c with QDs as indicated. QDs were stained with Hoechst 33342. Images were acquired from Z planes that best represent each structure using excitation and emission wavelengths at which the fluorescent channels are best excited and emitted. Bottom: 9.45-μm scale bar, 20 μm.

Green Fluorescent Protein

*Aequorea victoria* jellyfish

Osamu Shimomura

Shimomura O, Johnson F, Saiga Y (1962). "Extraction, purification and properties of aequorin, a bioluminescent protein from the luminous hydromedusan, *Aequorea*". *J Cell Comp Physiol* **59**: 223-39.

---

---

---

---

---

---

---

---

---

---

"The jellyfish *Aequorea* and its light-emitting organs"

O. SHIMOMURA: *Journal of Microscopy*, Vol. 217, Pt 1 January 2005, pp. 3–15



---

---

---

---

---


---

---

---

---

---



Intermolecular Energy Transfer in the Bioluminescent System of *Aequorea*†

Hiroshi Morise, Osamu Shimomura, Frank H. Johnson,\* and John Winant

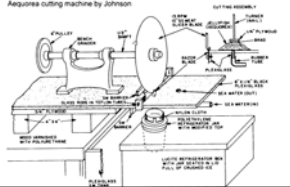
2656 BIOCHEMISTRY, VOL. 13, NO. 12, 1974

Materials and Methods

*Aequorin*. The material used in this study was extracted and purified from some 30,000 specimens of *Aequorea*

70 mgs of purified GFP were obtained. The 30,000 jellyfish weighed about 1.5 tons

The outer ring of the jellyfish had to be isolated. Initially scissors were used but then a "ring-cutting" machine was built



---

---

---

---

---

---

---

---

---

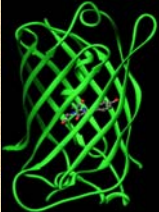
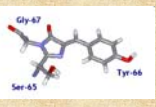
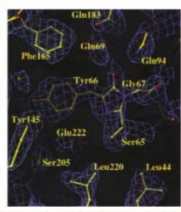
---

RESEARCH ARTICLE

© 1996 Nature Publishing Group: <http://www.nature.com/naturebiotechnology>

# The molecular structure of green fluorescent protein

Fan Yang, Larry G. Moss<sup>1</sup>, and George N. Phillips, Jr.\*

The GFP chromophore is formed via a posttranslational cyclization reaction involving the three amino acids serine 65, tyrosine 66 and glycine 67

---

---

---

---

---

---

---

---

---

---

This scenario was proposed in the paper that first presented the primary sequence of GFP

doi: 10.1101/229-233  
© 1992 Elsevier Science Publishers B.V. All rights reserved. 0378-1119/92/0005-00

0378-1119

## Primary structure of the *Aequorea victoria* green-fluorescent protein

(Bioluminescence; Cnidaria; apoptosis; energy transfer; chromophore; cloning)

Douglas C. Prasher<sup>a</sup>, Virginia K. Eckhardt<sup>a</sup>, William W. Ward<sup>a</sup>, Frank G. Prendergast<sup>a</sup> and Milton J. Curran<sup>a</sup>

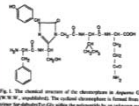


Fig. 1. The chemical structure of the chromophore in Aequorea GFP (Prasher et al., 1992). The chromophore is formed from the amino acids Ser65, Tyr66, and Gly67.

## THE GREEN FLUORESCENT PROTEIN

Roger Y. Tsien  
Howard Hughes Medical Institute, University of California, San Diego, La Jolla, CA 92037-0647

*Annu. Rev. Biochem.* 1998, 67:509-44  
Copyright © 1998 by Annual Reviews. All rights reserved

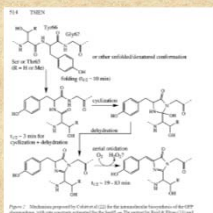


Fig. 1. The chemical structure of the chromophore in Aequorea GFP (Prasher et al., 1992). The chromophore is formed from the amino acids Ser65, Tyr66, and Gly67.

---

---

---

---

---

---

---

---

---

---

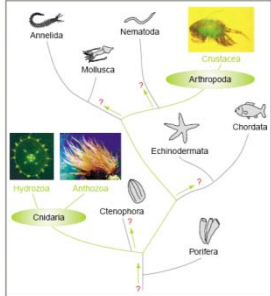


Figure 1. Phylogenetic relationship of the fluorescent protein-producing organisms on the phylogenetic tree. The phyla Cnidaria and Anthropoda (where GFP genes were found) and the branches connecting these phyla are highlighted in green. Photos show organisms representative of each phylum expressing GFP-like proteins: jellyfish *Physalia physalis* showing yellow fluorescence; sea anemone *Anemonia sulcata* with purple tentacle tips; and a copepod displaying green fluorescence. Question marks indicate possible, but unexplored, pathways of the evolution of FPs.

## Fluorescent proteins as a toolkit for *in vivo* imaging

Rebecca M. Zerkow, Susan L. Schmeissner and Elizabeth A. Lippman

---

---

---

---

---

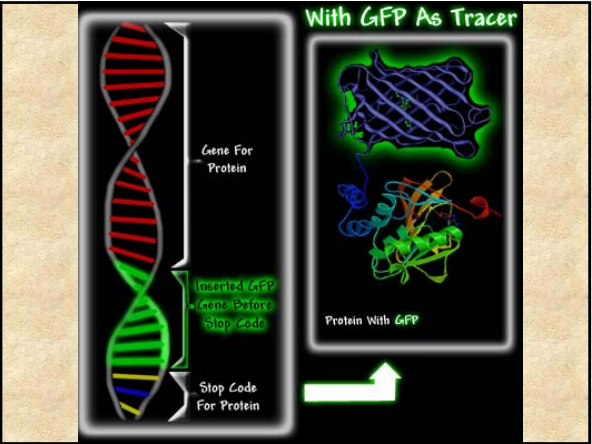
---

---

---

---

---



---

---

---

---

---

---

---

---



---

---

---

---

---

---

---

---

A number of new GFP proteins have been made using site directed mutagenesis to alter the amino acids near the chromophore and thus alter the absorption and fluorescence properties.

*Proc. Natl. Acad. Sci. USA*  
Vol. 91, pp. 12501-12504, December 1994  
Biochemistry

**Wavelength mutations and posttranslational autooxidation of green fluorescent protein**

(*Aequorea victoria*/blue fluorescent protein/*Escherichia coli*/lambdazitidine)

ROGER HEIM\*, DOUGLAS C. PRASHER<sup>†</sup>, AND ROGER Y. TS'EN\*<sup>‡</sup>

For all these reasons, it would be interesting to convert the *Aequorea* GFP excitation spectrum to a single peak, preferably at longer wavelengths. The cDNA was therefore subjected to random mutagenesis by hydroxylamine treatment or PCR. Approximately six thousand bacterial colonies on agar plates were illuminated with alternating 395- and 475-nm excitation and visually screened for altered excitation properties or emission colors. Although this number of colonies falls far short of saturating the possible mutations of a protein of 238 residues, interesting variants have already appeared.

WT GFP Blue mutant

← Tyr-66 replaced by His

---

---

---

---

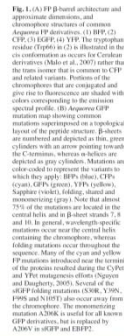
---

---

---

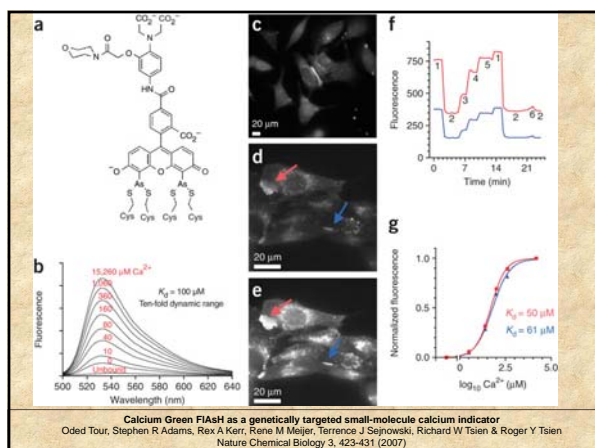
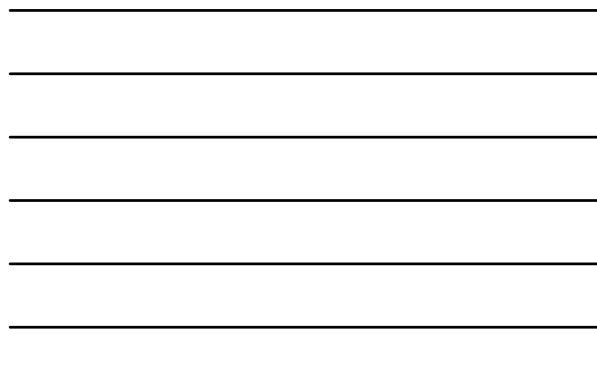
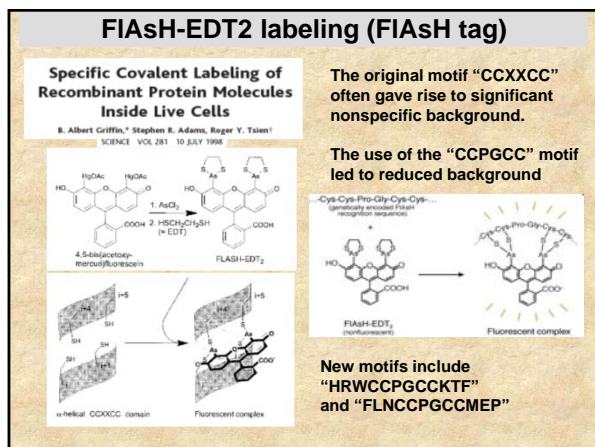
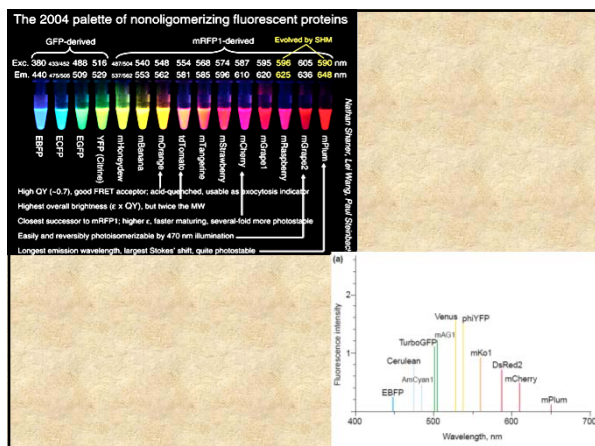
---



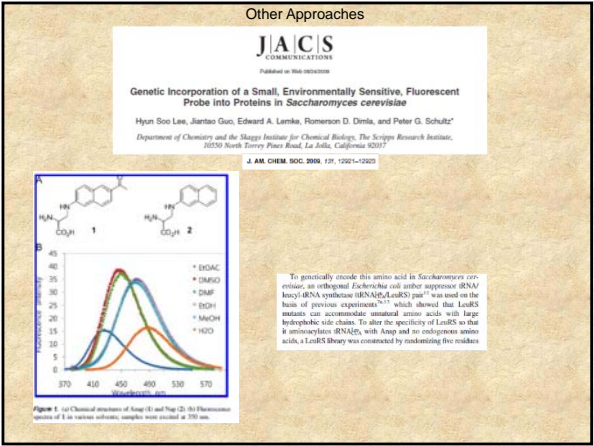
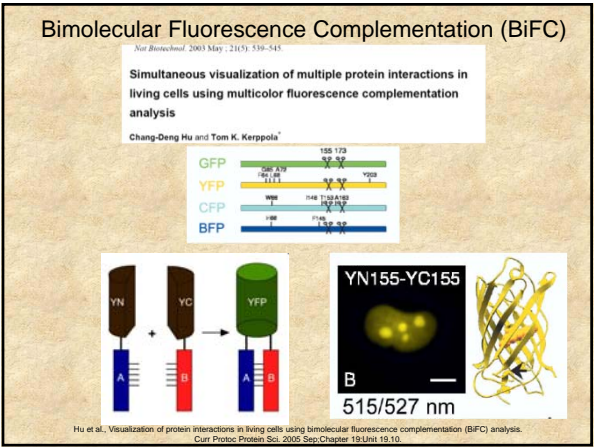
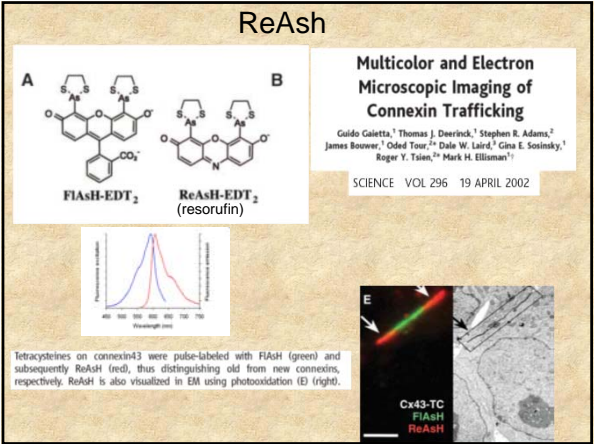


DsRed GFP









That's all!!!



---

---

---

---

---

---

---

---